*Grenze International Journal of Engineering and Technology, Jan Issue*

# Hyperspectral Image-based Land Cover Prediction using Improved Elman Network Model

R.Vasanthi[1] and Dr. D. Christopher Durairaj[2]
[1]Research Scholar, Research Centre in Computer Science, V.H.N.S.N. College, Virudhunagar, Virudhunagar District
E-mail: vasanthirnaidu@gmail.com
[2]Associate Professor, Research Centre in Computer Science, V.H.N.S.N. College, Virudhunagar, Virudhunagar District
Email: kesterkaran@gmail.com

***Abstract*—This work anticipates a novel approach for classifying hyperspectral images using the machine learning classification approach. The machine learning (ML) approach is used for classification without the intervention of humans. The classification accuracy through ML is improved by examining the input images. Here, an improved Elman classifier (IEC) model is used to classify the input hyperspectral images accurately. This IEC model is designed for classifying the land cover regions exactly and intends to give higher classification accuracy. The increased classifier performance is compared with various prevailing approaches Random Forest (RF), Decision Tree (DT), Logistic Regression (LR), k-Nearest Network (k-NN), and Support Vector Machine (SVM). The anticipated model is utilized to enhance the classification accuracy drastically. Here, the hyperspectral images are used to classify the urban regions. The simulation is done with MATLAB 2016b simulation environment, and the experimental outcome provides superior performance and establishes a trade-off between the prevailing approaches. The prediction accuracy of IEC is 98.99%, precision is 64.66%, recall is 99.88%, and F1-measure is 74.46% which is comparatively higher than other approaches.**

***Index Terms*— Hyper-spectral images, land cover region, Elman classifier, machine learning, and prediction accuracy.**

## I. INTRODUCTION

Generally, the classification of diverse regions of hyperspectral images has broader applications like land cover detection and mapping, wetland mapping, water resource detection, agricultural usage, regional and urban planning, geological information, and agricultural use [1]. Moreover, hyperspectral image classification is considered a tedious task is owing to its complexity [2]. Similarly, feature extraction plays a substantial role during the classification approach. When features are manually chosen with human intervention, then the efficiency is reduced during the classification process. Therefore, a classifier model with superior functionality needs to be adopted [3]. Here, feature extraction is not performed as the input images are higher resolution images. Thus, direct classification can be applied with initial pre-processing [4].

Machine learning is one of the productive approaches in Artificial Intelligence (AI) to learn the discriminative features devoid of any manual interventions. Jensen et al. [5] consider how ML approaches are adopted for classification purposes. Indeed, the learned features are highly feasible for lower-level feature representation and

*Grenze ID: 01.GIJET.8.1.130*

show higher significance in image classification like handwritten recognition, face recognition and scene classification. Farias et al. [6] discuss remote sensing images; various investigators involve themselves in image classification using ML approaches like SVM, k-NN, DT, RF, and LR. However, the feature extraction process is adopted for the 1D spectral feature, which is not appropriate for high-resolution image classification. Sano et al. [7] anticipate a learning approach by initiating spatial characteristics for reliable hyperspectral image classification in another work.

The Machine Learning (ML) approaches are popular for high-resolution image classification owing to their potential to explore spatial features, as stated by Abualigah et al. [8]. Moreover, ML is generally learned from pixel-based and local image patches that cause misleading or misinterpretations sometimes. As well, ML-based feature extraction does not offer a clear outline regarding edges and boundaries. Therefore, to handle these complexities, various object-based classification approaches are proposed by Baboo et al. [9] to delineate classification effectually with high-resolution images. Birhane et al. [10] consider object-based classification approaches for image segmentation, a building block for image analysis.

Carranza et al. [11] analyses various existing approaches to perform classification with LISS images. The author adopts wavelet packet transform for analyzing texture using LISS images. Here, co-occurrence and statistical features of the provided input patterns are extracted initially, and these features are utilized for classification purposes. The author considers Mahalanobis and Daubechies wavelet filters for decomposition and classification purposes. The outcomes of the classifier model possess various features; some of these predicted features are not resourceful. The superior features among the wavelet packet co-occurrence textural and wavelet packet statistical features are chosen to adopt the Genetic Algorithm (GA). The author considers some other feature reduction approaches like linear discriminant analysis and principal component analysis. Then, the multilayer perceptron layer is supposed for classification approaches. This classifier model outperforms various prevailing works when MLP is substituted with multiple adaptive neuro-fuzzy inference systems (ANFIS) trained with a back-propagation gradient model merged with the least square approach. However, these approaches fail to give better prediction accuracy. This research intends to enhance the prediction accuracy using a novel Improved Elman classifier (IEC) model. The anticipated model is adopted for the classification of hyperspectral images with the IEC model. Here, classification is performed uniquely to enhance the model efficiency. The proposed IEC model is used for classifying hyperspectral images. The model is more robust with more vital optimization, computational power and associative memory.

The work is organized as section 2 provides extensive analysis with various existing approaches; section 3 provides a detailed explanation regarding the dataset acquisition, pre-processing with data normalization and classification with the IEC model. In section 4, the numerical outcomes of the anticipated model are discussed. Section 5 shows the summary of the research with the extension of the future research idea.

## II. RELATED WORKS

This section provides a review of various existing approaches. Elatawneh et al. [12] discuss multiple factors influencing prediction accuracy, i.e. evaluation data accuracy, training source, sensor types, classification methods and several classes. With all these factors, the assortment of most appropriate algorithm that acquires dominant prediction accuracy with reduced processing time. This process is more crucial. Various approaches are anticipated to model remote sensing-based land cover mapping, and it includes both supervised and unsupervised methods and non-parametric and parametric models. Even though unsupervised techniques like k-means and the Data clustering model have been extensively utilized for the past few years, these clustering models are complex and cumbersome to perform the classification performance [13]. Similarly, parametric supervised approaches like multi-nominal logistic regression and linear discriminant analysis are also utilized broadly. The studies of these methods are performed in a standard manner. In the past few decades, non-parametric methods like k-NN, SVM, RF and so on have acquired the attention of researchers for remote-sensing based land cover mapping and classification. Moreover, both RF and SVM necessitate attribute selection with multiple parameters that influence efficiency, which is computationally complex and intensive. Heidarlou et al. [14] discuss the k-NN model, which reports complexity is choosing the optimal k-value, and the adopted GA model is suggested for the optimization model. Also, it is computationally intensive. At last, the object-based prediction and classification method is considered a superior method for categorizing fine-resolution images. John et al. [15] adopt object-based approaches merged with the NN and fuzzy set models for mapping land cover regions using satellite images. However, object-based classification approaches enhance the prediction accuracy for various remotely sensed spatial resolutions and cover mapping applications. It remains the most appropriately utilized data source for these kinds of applications. In summary, although only a few studies using only a few methods have been used to classify forest land in Vietnam, the reported accuracies are relatively large. Thus, there is merit in a more comprehensive evaluation of classification methods, particularly for diverse tropical regions such as in Dak Nong province, Vietnam, with their distinct seasonal effects.

The unique nature of every study or research area includes sample sizing, definitions and characteristics and numbers of classes. The comparison of these approaches is performed based on the prediction accuracy acquired with these studies. Although these methods do not pose much effort and evaluating these methods is complex for various forest regions. Kavzoglu et al. [16] adopt the LR model with LandSat images to evaluate different classes of forest regions and reports classification accuracy of 64% to 69%. The adoption of the RF model for land cover classification and various methods are reported. Kwan et al. [17] adopts both sentinel-2 and Landsat data for land cover variation classes and provides an overall prediction accuracy of 81%. Lin et al. [18] adopt Landsat data and RF model for ten classes with multiple forest classes in the Vietnam region. Here, the overall prediction accuracy is 90% accurately. Mhangara et al. [19] use Landsat data, and the RF model for seven land cover classes includes overall prediction accuracy and classification of land cover regions higher than 91%. At last, Mishra et al. [20] adopt the SVM model to attain higher prediction accuracy than RF for categorizing various land cover regions, including sentinel-2 data and river delta data. As a summary of this review, even though these studies adopt multiple methods for classifying the land cover regions, these prediction methods lack higher classification approaches [21] – [25]. Therefore, there is a need for an enhanced prediction model for classifying the land cover region. It is attained with the adoption of an improved ML approach over various tropical regions. Here, an Improved Elman classifier (IEC) model is used to classify the input hyperspectral images accurately.

## III. METHODOLOGY

This research includes three preliminary phases: data acquisition, pre-processing with data normalization, and classification with the IEC model. Here, the simulation is done with MATLAB 2016b environment and metrics like prediction accuracy is evaluated and compared with various existing approaches. Fig 1 depicts the workflow of the anticipated land cover prediction model.

### *A. Dataset description*

This research considers 220 Band AVIRIS Hyperspectral Image dataset for predicting land cover or land use region. It includes Indian Pine Test Site 3 with reference data, including observation photos and notes for fields with an approximately 20m spatial resolution. Airborne Visible/Infrared Imaging Spectrometer (AVIRIS) hyperspectral sensor data was acquired in June 1992 over Purdue University Agronomy farm of Western Lafayette and surrounding regions (Ref: https://purr.purdue.edu/publications/1947/1). The information is developed to help soil research conducted by Marion and his scholars. It includes a significant part of Indian Pine Creek and Creek watersheds, and thus it is termed the Indian Pine dataset. It contains two flight lines known as East-West flown and North-South flown. There are three approximately 2 miles by 2-mile intensive test suites in the northern portion of the North-South flight line, one in the southern part, and one near the centre. The field photos and notes of AVIRIS data are provided for site 3. Here, the residue is focussed, and photos and notes document of residue condition is provided for the fields. The image provided is 145*145*220 dimensions.

### *B. Data normalization*

It is a most general approach used for performing pre-processing. It converts the image values into a specific range, i.e. 0 and 1. The normalization approaches considered here are z-score normalization and zero means. It is expressed as in Eq. (1):

$$X_i' = \frac{X_i - mean\ (X)}{SD\ (X)} \tag{1}$$

Here, $X_i'$ is normalized data; $mean\ (X)$ specifies mean value, and $SD\ (X)$ specifies standard deviation of input X. The SD is mathematically expressed as in Eq. (2):

$$\sigma = \sqrt{\frac{1}{N-1}\sum_{i=1}^{N}\left(X_i - mean\ (X)\right)^2} \tag{2}$$

Here, $\sigma$ specifies the standard deviation for the provided input values.

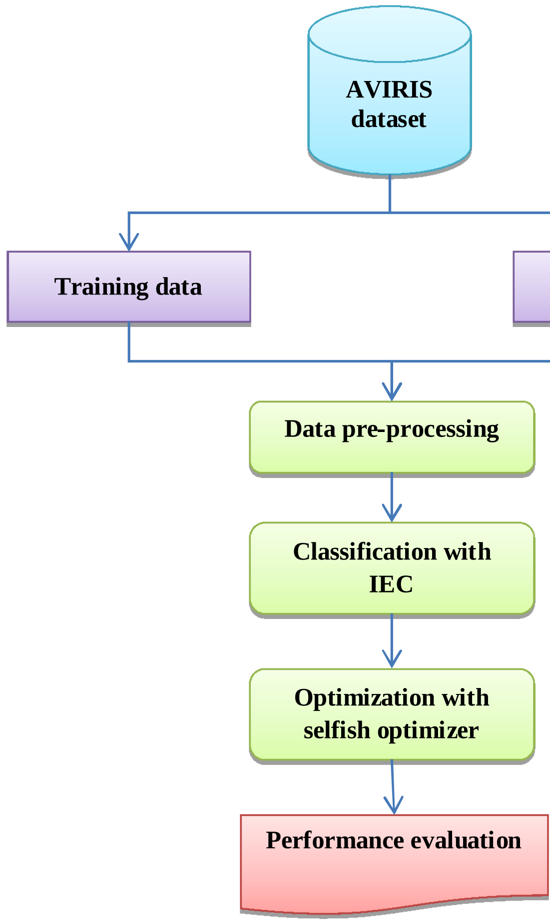


Fig 1. Workflow of proposed IEC land cover prediction model

*C. Improved Elman classifier model*

Here, the existing Elman network model is improved with the selfish optimization approach (SO). Then, the integrated model is coined as the Improved Elman classifier model. It is utilized for classifying the hyperspectral image. It is used for image classification and optimizing the weight of the network model. The number of image attributes is given as the input to the Elman network model. The proposed IEC model includes four diverse layers: the input layer, context layer, output layer, and hidden layer. The input is used to convert the raw input image; the context layer is used to preserve the output data from the previously hidden layers and provide a response based on the hidden layer. The functionality of the hidden layer is to map the weighted data via the transfer function. The processed data is provided in the output layer. The anticipated model possesses a temporary function and handles the complex input data. The proposed IEC model shows superior optimization computation, computational power, robust and associative memory. It is mathematically expressed as in Eq. (3) – Eq. (5):

$$x(t) = f\left(w_1 x_c(t) + w_2\left(u(t-1)\right)\right) \quad (3)$$

$$y(t) = g(w_3 x(t)) \quad (4)$$

$$x_c(t) = x(t-1) \quad (5)$$

Here, $x(t), y(t), x_c(t)$ specifies the $i^{th}$ hidden layer output, output and context layer. The input vector is depicted as $'u'$, $w_1$ specifies the connection weight (context layer) to the hidden layer; $w_2$ specifies the weighted value (input layer) to the hidden layer; $w_3$ determines the weighted value (hidden value) to the output layer, $f(.)$ specifies transfer function (hidden layer), and $g(.)$ defines the transfer function (output layer). For all iterations, feedback data is acquired from the hidden layer of the previous layer. It does not adopt spatial or temporal data ultimately. The improved network model considers the feedback output of both the context and hidden layer. The most prominent result is provided back to the network model as the sample data is comprehensively analyzed, and it is more suited for the classification process. It is mathematically expressed as in Eq. (6):

$$x_c(t) = x(t-1) + \propto x_c\ (t-1) \tag{6}$$

Here, $\propto$ specifies the scalar constant; the cross-entropy based loss function is expressed as in Eq. (7):

$$L\ (d, y) = -\sum_{j=1}^{N}[d_j(t) \log y_j\ (t) + \left(1 - d_j(t)\right) \log(1 - y_j(t))] \tag{7}$$

Here, $d_j(t)$ specifies the target of getting the essential information, and $y_j(t)$ determines the gained output. The proposed optimization approach is used for measuring the IEC weighted value. $w_1, w_2, w_3$ are depicted as the three essential weighted parameters of IEC. The weighted values are evaluated using the selfish optimizer. When compared to another optimizer, the proposed model shows superior convergence speed, lower computational time and lower computational complexity. The functionality of the anticipated model is given below. The selfish optimizer is a famous meta-heuristic optimizer that integrates the activities of both the fish and sardine. Here, fish acts as a predator, and the sardine plays the role of prey. This optimizer is determined explicitly as a social predator as it forms the group to catch the prey. In this hunting activity, various strategies are adopted for hunting the prey. Here, the provided population (fish) attack the sardine group and hunts them; however, some hunters preserve their power. The group of fish that performs the hunting operation updates its position, and the sardine also updates the position over the vacant space. It is committed to escape them from the attack. This position changing process is performed after the member of the group gets attacked. The updated location of the fish is expressed as in Eq. (8), where it includes the population initialization, maximal number of iterations and coefficient values.

$$x^i_{new}\ (fish) = x^i_{best} - \lambda_i * \left( \propto * \left( \frac{x^i_{elite} + x^i_{injured\ sardine}}{2} \right) - x_{old(sardine)} \right) \tag{8}$$

Here, the position (best) of the sardine is specified as $x^i_{best}$, the injured sardine position is specified as $x^i_{injured\ sardine}$, current sardine position is expressed as $x_{old(sardine)}$ and $\propto$ specifies the random number 1 and 0, $\lambda_i$ specifies coefficient values. It is expressed as in Eq. (9):

$$\lambda_i = \left(2 * \propto * density_{prey}\right) - density_{prey} \tag{9}$$

Here, $density_{prey}$ specifies the density of prey. During the hunting process, the number of prey reduces. For this cause, the prey density is essential for enhancing the fish location around the sardine. The prey density parameter is mathematically expressed as in Eq. (10):

$$Density_{prey} = 1 - (N_f / N_f + N_s) \tag{10}$$

Here, $N_f$ specifies the number of fish, and $N_s$ specifies the number of sardines. The new sardine position is evaluated using Eq. (11):

$$x^i_{new_{sardine}} = r * (x^i_{best\ position} - x^i_{old\ (sardine)} + power_{attack} \tag{11}$$

Here, the current position of sardine is provided as $x^i_{old\ (sardine)}$; $r$ is an arbitrary number among 0 and 1. The attack power of the fish is expressed as in Eq. (12):

$$Power_{attack} = A * (1 - 2 * iterations * \varepsilon)) \tag{12}$$

Here, numbers of iterations are called $iterations$, $A$ and $\varepsilon$ specifies the factor that reduces the attack power value. The sardine strategies are enhanced with Eq. (13):

$$\eta = power_{attack} * N_s \tag{13}$$

The power attack is less than 0.5, which helps in location modernization. When the attack power is higher than 0.5, then the sardine is updated. When the sardine fits the fish population, then it is best suited for prey attack. Based on these conditions, enhance the chance of new prey chasing, the fish location is altered based on the unique position of sardine. It is expressed as in Eq. (14):

$$X_f^i = X_{sardine}^i ; \quad if\ f(S_i) < f(f_i) \tag{14}$$

Based on Eq. (14), the average fish value and sardine position are specifically considered for weight calculation. The mean values of these positions are taken from the IEC model. The mean value is expressed as in Eq. (15):

$$mean = \frac{Position_f + position_s}{2} \tag{15}$$

This process is repeated until the fulfilment of the termination condition.

## IV. NUMERICAL RESULTS AND DISCUSSION

This section shows the experimental result of the anticipated model using MATLAB 2016b simulation environment with a PC configuration of i5 processor, 1.90 GHz and 4 GB RAM. Some performance metrics considered for the prediction purpose are accuracy, precision, recall, and F-measure. The performance of the anticipated model is compared with RF, SVM, DT, LR and k-NN. The performance indicators are provided based on the confusion matrix where $TP$ specifies the number of instances predicted as positive and considered to be positive actually; $TN$ specifies the number of instances predicted to be negative that are negative actually; $FP$ specifies the number of instances that are negative actually but intends to be positive, and $FN$ specifies the number of positive instances is intended to be negative. Here, the land cover prediction accuracy entirely relies on the ability of the model to handle the complete instance as negative or positive. It is expressed as below:

$$Prediction\ accuracy = \frac{(TP + TN)}{(TP + FN + FP + TN)} * 100\% \tag{16}$$

**Precision** is depicted as the proportion of appropriately predicted positive instances out of all positive predictions provided by the predictor model. It is expressed as in Eq. (17):

$$Precision = \frac{TP}{(TP + FP)} \tag{17}$$

**The recall** is depicted as the proportion of predicted positive instances to be positive always. It is expressed as in Eq. (18):

$$Recall = \frac{TP}{(TP + FN)} \tag{18}$$

**F1-score** is depicted as the measure generally used for classification problems. It adopts the average harmonic method to determine the recall and precision rate where the maximal value is set as 1, and the minimum value is set as 0. It is mathematically expressed as in Eq. (19):

$$F1 - score = 2 * \frac{precision * recall}{precision + recall} \tag{19}$$

Fig 1 to Fig 3 depicts the outcome of the anticipated IEC model. Table 1 compares the proposed IEC model with existing RF, DT, LR, SVM, and k-NN. Here, metrics like accuracy, precision, recall and F-measure are evaluated. The prediction accuracy of IEC is 98.99% which is 23.43%, 22.07%, 19.93%, 18.62% and 16.27% higher than DT, LR, k-NN, RF and SVM. The precision of IEC is 64.66% which is 19.11%, 17.67%, 15.22%, 13.6% and 10.51% higher than DT, LR, k-NN, RF and SVM. The recall of IEC is 99.88% which is 19.26%, 18.26%, 16.69%, 15.76%, and 14.1% higher than DT, LR, k-NN, RF and SVM. The F-measure of IEC is 74.46% which is 23.77%, 52.11%, 20.09%, 18.62% and 15.97% higher than DT, LR, k-NN, RF and SVM (See Fig 5). From the analysis, it is noted that the anticipated model shows higher performance than the existing approaches.

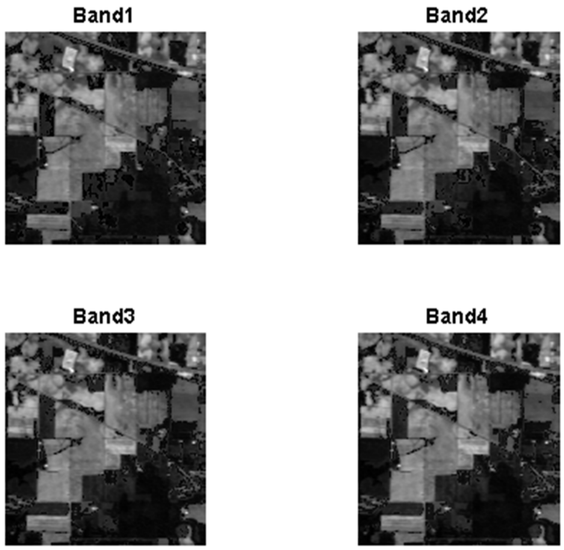


Fig 2 Input image

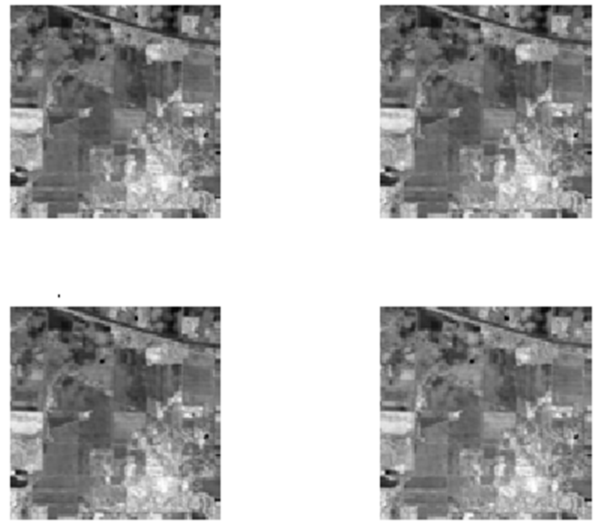

Fig 3 Pre-processed image

Fig 4 Classified image

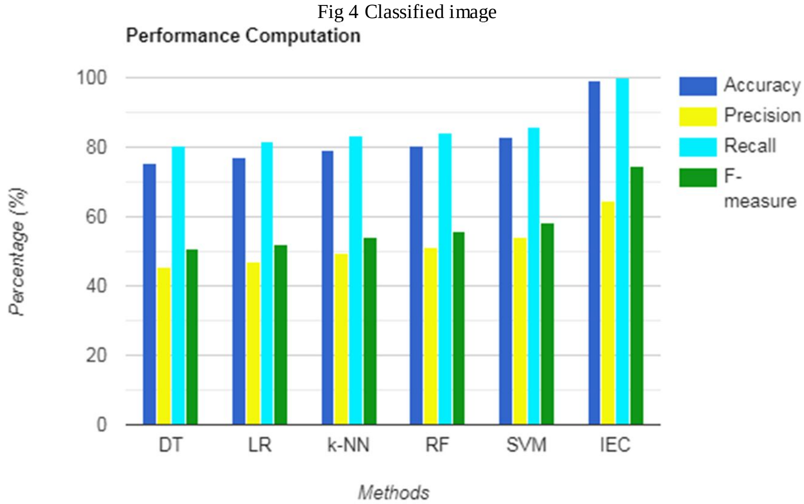


Fig 5 Comparison of performance evaluation

TABLE I. PERFORMANCE EVALUATION OF PROPOSED VS EXISTING METHODS

| **Metrics** | **DT** | **LR** | **k-NN** | **RF** | **SVM** | **IEC** |
|---|---|---|---|---|---|---|
| **Accuracy** | 75.56% | 76.92% | 79.06% | 80.37% | 82.72% | **98.99%** |
| **Precision** | 45.55% | 46.99% | 49.44% | 51.06% | 54.15% | **64.66%** |
| **Recall** | 80.62% | 81.62% | 83.19% | 84.12% | 85.78% | **99.88%** |
| **F-measure** | 50.77% | 52.11% | 54.37% | 55.84% | 58.49% | **74.46%** |

## V. CONCLUSION

This research provides extensive analysis with the land cover region prediction using hyperspectral images. It offers a generic outcome with the anticipated improved Elman classifier (IEC) model used for accurately classifying the input hyperspectral images. This IEC model is designed to automatically integrate selfish optimizers for classifying the land cover regions and intends to give higher classification accuracy. Here, the input is taken from the AVIRIS Hyperspectral Image dataset, and the pre-processing is done with data normalization. It is followed by classification with the proposed IEC model. The simulation is done with MATLAB 2016b environment where various metrics like accuracy, precision, recall and F1-measure are computed and compared with multiple prevailing approaches like RF, DT, LR, SVM and k-NN model. The prediction accuracy of IEC is 98.99%, precision is 64.66%, recall is 99.88%, and F1-measure is 74.46% which is comparatively higher than other approaches. The anticipated model provides superior classification outcomes and establishes a better trade-off among the existing approaches. The target of this research is to motivate the upcoming researchers to perform land cover prediction competently. It helps the urban management, resource planners, government officials, and forest departments take official actions to preserve the earth's environmental condition.

## REFERENCES


[1] Bounouh, H. Essid, and I. R. Farah. “Prediction of land use/land cover change methods: A study. En advanced technologies for signal and image processing (ATSIP),” in Proc. Int. Conf. IEEE, 2017, p. 1–7

[2] Pijanowski, D. G. Brown, B. A. Shellito, and G. A. Manik. "Using neural networks and GIS to forecast land-use changes: a land transformation model,” Comput., Environ. urban Syst., vol. 26, no. 6, pp. 553–575, 2002

[3] Verburg, P. P. Schot, M. J. Dijst, and A. Veldkamp, “Land use change modelling: Current practice and research priorities,” Geojournal, vol. 61, pp. 309–324, 2004.

[4] Lu, X. J. Huang, T. H. Zuo, S. S. Xiao, X. F. Zhao, and X. Y. Zhang, “Land use scenarios simulation based on CLUE-S and Markov composite model—A case study of Taihu lake rim in Jiangsu province,” Sci. Geol. Sinica, vol. 29, pp. 577–581 2009.

[5] Jensen, “Remote sensing the urban landscape,” in Remote Sensing of the Environment: An Earth Resource Perspective, 2nd ed. India: Pearson Education India, 2009, ch. 13, pp. 525–589.

[6] Farias, A. Marquez, E. Guevara, D. Rey, “Characterization spatiotemporal land use in a watershed using geomatic techniques,” Revista Ingenieria UC, vol. 25, no. 1, pp. 19–30, Apr. 2018.

[7] Sano, L. G. Ferreira, G. P. Asner, and E. T. Steinke, "Spatial and temporal probabilities of obtaining cloud-free Landsat images over the Brazilian tropical savanna,” Int. J. Remote Sens., vol. 28, no. 12, pp. 2739– 2752, 2007

[8] Abualigah LM, Khader AT (2017) Unsupervised text feature selection technique based on hybrid particle swarm optimization algorithm with genetic operators for the text clustering. J Supercomput 73(11):4773– 4795

[9] Babu SS, Renuka Devi M (2011) Geometric correction in recent high-resolution satellite imagery: a case study in Coimbatore, Tamil Nadu. Int J Comput Appl 14(1):32–37

[10] Birhane E, Ashfare H, Fenta AA, Hishe H, Gebremedhin MA, G. wahed H, Solomon N (2019) Land use land cover changes along topographic gradients in Hugumburda national forest priority area, northern Ethiopia. Remote Sensing Applications: Society and Environment 13:61–68

[11] Carranza-García M, García-Gutiérrez J, Riquelme JC (2019) A framework for evaluating land use and land cover classification using convolutional neural networks. Remote Sens 11(3):274

[12] Elatawneh A, Kalaitzidis C, Petropoulos GP, Schneider T (2014) Evaluation of diverse classification approaches for land use/cover mapping in a Mediterranean region utilizing Hyperion data. International Journal of Digital Earth 7(3):194–216

[13] Etemadi H, Smoak JM, Karami J (2018) Land use change assessment in coastal mangrove forests of Iran utilizing satellite imagery and CA–Markov algorithms to monitor and predict future change. Environ Earth Sci 77(5):208

[14] Heidarlou HB et al. (2019) Effects of preservation policy on land-use changes in Iranian northern Zagros forests. Land Use Policy 81:76–90

[15] John J, Chithra NR, Thampi SG (2019) Prediction of land use/cover change in the Bharathapuzha river basin, India using geospatial techniques. Environmental monitoring and assessment 191(6):354

[16] Kavzoglu T, Tonbul H, Yildiz Erdemir M, Colkesen I (2018) Dimensionality reduction and classification of hyperspectral images using object-based image analysis. Journal of the Indian Society of Remote Sensing 46(8):1297–1306
[17] Kwan C (2019) Methods and challenges using multispectral and Hyperspectral images for practical change detection applications. Information 10(11):353
[18] Lin C, Wu C-C, Tsogt K, Ouyang Y-C, Chang C-I (2015) Effects of atmospheric correction and pansharpening on LULC classification accuracy using WorldView-2 imagery. Information Processing in Agriculture 2(1):25–36
[19] Mhangara P, Odindi J (2013) Potential of texture-based classification in urban landscapes using multispectral aerial photos. S Afr J Sci 109(3–4):1–8
[20] Mishra, Varun Narayan, et al. (2016). "Evaluation of land use/land cover classification accuracy using multi-resolution remote sensing images." Forum geographic. Vol. 15. No. 1. The University of Craiova, Department of Geography
[21] Mustafa, Elhadi K, et al. (2019). "Simulation of land use dynamics and impact on land surface temperature using satellite data." GeoJournal.: 1–19
[22] Papadomanolaki, Maria, et al. (2019). "Detecting urban changes with recurrent neural networks from multitemporal Sentinel-2 data." IGARSS 2019–2019 IEEE International Geoscience and Remote Sensing Symposium.
[23] Qin H-p, Yi W-n, Ma J-j, Ding X-x, Zhu X-b (2013) Topographic imaging simulation of optical remote sensing based on Landsat TM data. Optik 124(7):586–589
[24] Sawant, Shrutika S., and M. Prabukumar (2017). "Semi-supervised techniques based hyperspectral image classification: a survey." 2017 Innovations in Power and Advanced Computing Technologies (i-PACT).
[25] Sertel E, Alganci U (2016) Comparison of pixel and object-based classification for burned area mapping using SPOT-6 images. Geomatics, Natural Hazards and Risk 7(4):1198–1206